

# Additive Dose Response Models: Defining Synergy

Simone Lederer<sup>1</sup>, Tjeerd M.H. Dijkstra<sup>2,3</sup>, and Tom Heskes<sup>1</sup>

<sup>1</sup>Data Science, Institute for Computing and Intelligent Systems, Radboud University, Postbus 9010, 6500 GL Nijmegen, The Netherlands

<sup>2</sup>Max Planck Institute for Developmental Biology, Max-Planck-Ring 1, 72076 Tübingen, Germany

<sup>3</sup>Center for Integrative Neuroscience, University Clinic Tübingen, Otfried-Müller-Str. 25, 72076 Tübingen, Germany

November 26, 2018

## Abstract

*In synergy studies, one focuses on compound combinations that promise a synergistic or antagonistic effect. With the help of high-throughput techniques, a huge amount of compound combinations can be screened and filtered for suitable candidates for a more detailed analysis. Those promising candidates are chosen based on the deviance between a measured response and an expected non-interactive response. A non-interactive response is based on a principle of no interaction, such as Loewe Additivity [Loewe, 1928] or Bliss Independence [Bliss, 1939]. In Lederer et al. [2018], an explicit formulation of the hitherto implicitly defined Loewe Additivity has been introduced, the so-called Explicit Mean Equation. In the current study we show that this Explicit Mean Equation outperforms the original implicit formulation of Loewe Additivity and Bliss Independence when measuring synergy in terms of the deviance between measured and expected response. Further, we show that a deviance based computation of synergy outperforms a parametric approach. We show this on two datasets of compound combinations that are categorized into synergistic, non-interactive and antagonistic [Yadav et al., 2015, Cokol et al., 2011].*

**Keywords:** *synergy, Loewe Additivity, Bliss Independence, dose equivalence, Combination Index, General Isobole Equation, Explicit Mean Equation, Hill curve, null reference model, response surface, lack-of-fit*

## 1 Introduction

When combining a substance with other substances, one is generally interested in interaction effects. Those interaction effects are usually described as synergistic or antagonistic, dependent on whether the interaction is positive, resulting

26 in greater effects than expected, or negative, resulting in smaller effects than  
27 expected. From data generated with high-throughput techniques, one is con-  
28 fronted with massive compound interaction screens. From those screens, one  
29 needs to filter for interesting candidates that exhibit an interaction effect. To  
30 quickly scan all interactions, a simple measure is needed. Based on that pre-  
31 processing scan, those filtered combination candidates can then be examined in  
32 greater detail.

33 To determine whether a combination of substances exhibits an interaction  
34 effect, it is crucial to determine a non-interactive effect. Only when deviance  
35 from that so-called null reference is observed, can one speak of an interactive  
36 effect [Lederer et al., 2018]. Over the last century, many principles of non-  
37 interaction have been introduced. For an extensive overview, refer to [Greco  
38 et al., 1995, Geary, 2012]. Two main principles for non-interactivity have sur-  
39 vived the critics: Loewe Additivity [Loewe, 1928] and Bliss Independence [Bliss,  
40 1939]. The popularity of Loewe Additivity is based on its principle of sham com-  
41 bination which assumes no interaction when a compound is combined with itself.  
42 Other null reference models do not hold that assumption. An alternative is Bliss  
43 Independence, which assumes (statistical) independence between the combined  
44 compounds.

45 Independent of the indecisive opinions about the null reference, there are  
46 multiple proposals how synergy can be measured given a null reference model.  
47 Some suggest to measure synergy as the difference between an observed isobole  
48 and a reference isobole calculated from a null-reference model. An isobole is  
49 the set of all dose combinations of the compounds that reach the same fixed  
50 effect, such as 50% of the maximal effect [Minto et al., 2000, Chou and Talalay,  
51 1984]. Another way to quantify synergy on the basis of the isobole is to look at  
52 the curvature and arc-length of the longest isobole spanned over the measured  
53 response [Cokol et al., 2011]. As the deviation from an isobole is measured for a  
54 fixed effect or dose ratio, synergy is only measured locally along that fixed effect  
55 or dose ratio. In order to not miss any effects, this method has to be applied  
56 for as many dose ratios possible.

57 In this paper we measure synergy as the deviation over the entire response  
58 surface. One way to do so is the Combenefit method by measuring synergy  
59 in terms of volume between the expected and measured effect [Di Veroli et al.,  
60 2016]. We will refer to it as a lack-of-fit method as it quantifies the lack of fit from  
61 the measured data to the null reference model. Another way of capturing the  
62 global variation is by introducing a synergy parameter  $\alpha$  into the mathematical  
63 formulation of the response surface. This parameter  $\alpha$  is fitted by minimizing  
64 the error between the measured effect and the  $\alpha$ -dependent response surface.  
65 Such statistical definition of synergy allows for statistical testing of significance  
66 of the synergy parameter. The cost of this more statistical approach is the  
67 complexity of the model fits.

68 As the research area of synergy evolved from different disciplines, different  
69 terminologies are in common use. The response can be measured among others  
70 in growth rate, survival, or death. It is usually referred to as the measured or  
71 phenotypic effect or as cell survival. In this study we interchange the terms  
72 response and effect.

73 When measuring a compound combination, one also measures each agent  
74 individually. The dose or concentration is typically some biological compound  
75 per unit of weight when using animal or plant models or per unit of volume

when using a cell-based assay. However, it can also be an agent of a different type for example a dose of radiation as used in modern combination therapies for cancer [Nat, 2018]. This individual response is called mono-therapeutic response [Di Veroli et al., 2016] or single compound effect. We prefer a more statistical terminology and refer to it as conditional response or conditional effect. With record we refer to all measurements taken of one cell line or organism which is exposed to all combinations of two compounds. In other literature, this is referred to as response matrix [Lehar et al., 2007, Yadav et al., 2015].

In Section 2.1, we give a short introduction to the two null response principles, Loewe Additivity and Bliss Independence. We explain in detail several null reference models that build on those principles. We introduce synergy as any effect different from an interaction free model in Section 2.2. There, we also introduce the parametrized and deviance based synergy approaches. In Section 2.3, we introduce two datasets that come with a categorization into synergistic, non-interactive and antagonistic. We evaluate the models and methods in Section 3 together with a detailed comparison of the synergy scores.

## 2 Materials and Methods

### 2.1 Theory

Before one can decide whether a compound combination exhibits a synergistic effect, one needs to decide on the expected effect assuming no interaction between the compounds. Such so-called null reference models are constructed from the conditional (mono-therapeutic) dose-response curves of each of the compounds, which we denote by  $f_j(x_j)$  for  $j \in \{1, 2\}$ . Null reference models extend the conditional dose-response curves to a (null-reference) surface spanned between the two conditional responses. We denote the surface as  $f(x_1, x_2)$  such that

$$f(x_1, 0) = f_1(x_1) \tag{1}$$

and

$$f(0, x_2) = f_2(x_2). \tag{2}$$

Thus, the conditional response curves are the boundary conditions of the null reference surface. For this study, we focus on Hill curves to model the conditional dose-responses. More detailed information can be found in Appendix A.

#### 2.1.1 Loewe Additivity

Loewe Additivity builds on the concepts of sham combination and dose equivalence. The first concept is the idea that a compound does not interact with itself. The latter concept assumes that both compounds that reach the same effect can be interchanged. Therefore, any linear combination of fractions of those doses which reach the effect individually and, summed up, are equal to one, yields that exact same effect. Mathematically speaking, if dose  $x_1^*$  from the first compound reaches the same effect as dose  $x_2^*$  from the second compound, then any dose combination  $(x_1, x_2)$ , for which

$$\frac{x_1}{x_1^*} + \frac{x_2}{x_2^*} = 1 \tag{3}$$

117 holds, should yield the same effect as  $x_1^*$  and  $x_2^*$ . As this idea can be generalized  
118 to any effect  $y$ , one gets

$$119 \quad \frac{x_1}{f_1^{-1}(y)} + \frac{x_2}{f_2^{-1}(y)} = 1, \quad (4)$$

120 where  $x_1^*$  and  $x_2^*$  are replaced with  $f_1^{-1}(y)$  and  $f_2^{-1}(y)$ , the inverse functions  
121 of Hill curves, respectively. For a fixed effect  $y$ , Eq. 4 defines an isobole, which  
122 is in mathematical terms a contour line. Hence the name of this model: the  
123 General Isobole Equation. It is an implicit formulation as the effect  $y$  of a dose  
124 combination  $(x_1, x_2)$  is implicitly given in Eq. 4. In the following we use the  
125 mathematical notation for the General Isobole Equation  $f_{GI}(x_1, x_2) = y$  with  
126  $y$  being the solution to Eq. 4.

127 It was shown by Lederer et al. [2018] that the principle of Loewe Additivity  
128 is based on a so-called Loewe Additivity Consistency Condition (LACC). This  
129 condition is that it should not matter whether equivalent doses of two com-  
130 pounds are expressed in terms of the first or the second. Under the assumption  
131 of the LACC being valid, Lederer et al. [2018] have shown, that a null reference  
132 model can be formulated explicitly, by expressing the doses of one compound in  
133 terms of the other compound:

$$134 \quad f_{2 \rightarrow 1}(x_1, x_2) = f_1(x_1 + f_1^{-1}(f_2(x_2))) \quad (5)$$

$$135 \quad f_{1 \rightarrow 2}(x_1, x_2) = f_2(f_2^{-1}(f_1(x_1)) + x_2), \quad (6)$$

137 where  $f_1^{-1}(f_2(x_2))$  is the dose  $x_1$  of compound one to reach the same effect of  
138 compound two with dose  $x_2$  (see Fig. 7 in Appendix A). Summing up this dose  
139 equivalent of the first compound with the dose of the first compound allows for  
140 the computation of the expected effect of the compound combination. With  
141 the two formulations above, the effect  $y$  of the dose combination  $(x_1, x_2)$  is  
142 expressed as the effect of either one compound to reach that same effect. Under  
143 the LACC, all three models, Eq. 4, Eq. 5 and Eq. 6 are equivalent. It was  
144 further shown, that, in order for the LACC to hold, conditional dose-response  
145 curves must be proportional to each other. It has been commented by Geary  
146 [2012] and shown in [Lederer et al., 2018], that this consistency condition is  
147 often violated. In an effort to take advantage of the explicit formulation and  
148 to counteract the different behaviour of Eq. 5 and Eq. 6 in case of a violated  
149 LACC, Lederer et al. [2018] introduced the so-called Explicit Mean Equation as  
150 mean of the two explicit formulations of Eq. 5 and Eq. 6:

$$151 \quad f_{\text{mean}}(x_1, x_2) = 1/2(f_{2 \rightarrow 1}(x_1, x_2) + f_{1 \rightarrow 2}(x_1, x_2)). \quad (7)$$

152 A more extensive overview of Loewe Additivity and definition of null reference  
153 models can be found in Lederer et al. [2018].

### 154 2.1.2 Bliss Independence

155 Bliss Independence assumes independent sites of action of the two compounds  
156 and was introduced a decade later than Loewe Additivity in [Bliss, 1939]. Note  
157 that the formulation of Bliss Independence depends on the measurement of the  
158 effect. The best known formulation of Bliss Independence is based on monoton-  
159 ically increasing responses for increasing doses:

$$160 \quad g_{\text{bliss}}(x_1, x_2) = g_1(x_1) + g_2(x_2) - g_1(x_1)g_2(x_2), \quad (8)$$

where  $g_i(x_i) = 1 - f_i(x_i)$  is a conditional response curve with increasing effect for increasing doses. In case the effect is measured in percent, i.e.  $y \in [0, 100]$ , the interaction term needs to be divided by 100 to ensure the right dimensionality of the term.

Here, we measure the effect in terms of cell death or growth inhibition. Therefore the conditional response curves are monotonically decreasing for increasing concentrations or doses.

$$f_{\text{bliss}}(x_1, x_2) = f_1(x_1) f_2(x_2). \quad (9)$$

The records are normalized to the response at  $x_1 = 0, x_2 = 0$ , thus  $f_1(0) = f_2(0) = 1$ . To arrive from Eq. 8 to Eq. 9, one replaces any  $g$  by  $1 - f$ . Chou and Talalay [1984] derive the Bliss Independence from a first order Michaelis-Menten kinetic system with mutually non-exclusive inhibitors.

## 2.2 Methods

The models introduced in the previous section are null reference models in that they predict a response surface in the absence of compound interaction. We capture synergy in a single parameter to facilitate the screening process. This is different from other approaches, such as Chou and Talalay [1977], who measure synergy as deviation from a null-reference isobole without summarizing the deviation in a single parameter. The single parameter value is typically referred to as synergy- or  $\alpha$ -score [Berenbaum, 1977]. As we investigate two methods to quantify synergy, we introduce two synergy parameters  $\alpha$  and  $\gamma$ , which measure the extent of synergy. Both synergy scores  $\alpha$  and  $\gamma$  are parametrized such that  $\alpha = 0$  or  $\gamma = 0$  denote absence of an interaction effect. In case  $\alpha$  or  $\gamma$  take a value different from zero, we speak of a non-additive, or interactive effect. A compound combination is, dependent on the sign of synergy parameter, one of the three following:

$$\alpha, \gamma \begin{cases} > 0 & \text{synergistic} \\ = 0 & \text{additive or non-interactive} \\ < 0 & \text{antagonistic} \end{cases} \quad (10)$$

Here, we measure synergy in two different ways, namely in fitting parametrized models or computing the lack-of-fit. The first method fits null reference models that are extended with a synergy parameter  $\alpha$ . For these parametrized models  $\alpha$  is computed by minimizing the square deviation between the measured response and the response spanned by the  $\alpha$ -dependent model. For the second method the difference between a null reference model and the data is computed. For this method, the synergy score  $\gamma$  is defined as the volume that is spanned between the null reference model and the measured response.

Just as the conditional responses form the boundary condition for the null-reference surface (Eq. 1, Eq. 2), we want the conditional responses to be the boundary condition for all values of  $\alpha$ . Explicitly, assuming a synergy model dependent on  $\alpha$  is denoted by  $f(x_1, x_2|\alpha)$ , then

$$\left. \begin{aligned} f(x_1, 0|\alpha) &= f_1(x_1) \\ f(0, x_2|\alpha) &= f_2(x_2) \end{aligned} \right\} \forall \alpha, \quad (11)$$

202 with  $f_i$  denoting the conditional response of compound  $i$ . We refer to Eq. 11 as  
203 the Synergy Desideratum. As we will see below, not all synergy models fulfill  
204 this property.

### 205 2.2.1 Parametrized Synergy

206 We extend the null reference models introduced in Section 2.1 in Eq. 4 - Eq. 9 to  
207 parametrized synergy models. The extension of the General Isobole Equation  
208 is the popular Combination Index introduced by Berenbaum [1977] and Chou  
209 and Talalay [1984]:

$$210 \quad \frac{x_1}{f_1^{-1}(y)} + \frac{x_2}{f_2^{-1}(y)} = 1 - \alpha. \quad (12)$$

211 Berenbaum originally equated the left-hand side of Eq. 4 to the so-called Com-  
212 bination Index  $I$ . Depending on  $I$  smaller, larger, or equal to 1, synergy, antag-  
213 onism or non-interaction is indicated. For consistency with the other synergy  
214 models, we set  $I = 1 - \alpha$  such that  $\alpha$  matches the outcomes as listed in Eq. 10. In  
215 Section 3 we will refer to this model as  $f_{\text{CI}}(x_1, x_2|\alpha)$ , where  $\alpha$  is the parameter  
216 that minimizes the squared error between measured data and Eq. 12.

217 Note that this model violates the Synergy Desideratum in Eq. 11 as  $\alpha$  not  
218 zero leads to deviations from the conditional responses. Explicitly,  $f_{\text{CI}}(x_1, 0|\alpha) =$   
219  $f_1((1 - \alpha)x_1) \neq f_1(x_1)$ . Although the Combination Index model violates the  
220 Synergy Desideratum, in practice it performs quite well and is in widespread  
221 use.

222 The explicit formulations in Eq. 5 and Eq. 6 are equivalent to the General  
223 Isobole Equation,  $f_{\text{GI}}(x_1, x_2)$ , given in Eq. 4, under the LACC [Lederer et al.,  
224 2018], but different if the conditional responses are not proportional. The two  
225 explicit equations are in fact an extension of the ‘cooperative effect synergy’  
226 proposed by Geary [2012] for compounds with qualitatively similar effects. For  
227 these explicit formulations in Eq. 5 and Eq. 6 we propose a model that captures  
228 the interaction based on the explicit formulations:

$$229 \quad f_{2 \rightarrow 1}(x_1, x_2|\alpha) = f_1(x_1 + (1 + x_1\alpha)f_1^{-1}(f_2(x_2))) \quad (13)$$

$$230 \quad f_{1 \rightarrow 2}(x_1, x_2|\alpha) = f_2((1 + x_2\alpha)f_2^{-1}(f_1(x_1)) + x_2). \quad (14)$$

232 With this, we can extend the Explicit Mean Equation model  $f_{\text{mean}}(x_1, x_2)$  in  
233 Eq. 7 to a parametrized synergy model:

$$234 \quad f_{\text{mean}}(x_1, x_2|\alpha) = 1/2(f_{2 \rightarrow 1}(x_1, x_2|\alpha) + f_{1 \rightarrow 2}(x_1, x_2|\alpha)), \quad (15)$$

235 which we refer to as  $f_{\text{mean}}(x_1, x_2|\alpha)$ . By multiplying the synergy parameter  
236  $\alpha$  with the dose we ensure that  $f_{\text{mean}}(x_1, 0|\alpha) = f_1(x_1)$  and  $f_{\text{mean}}(0, x_2|\alpha) =$   
237  $f_2(x_2)$ . Thus, the  $f_{\text{mean}}(x_1, x_2|\alpha)$  model fulfills the Synergy Desideratum (Eq. 11).

238 To investigate the difference between the two models  $f_{2 \rightarrow 1}(x_1, x_2)$  (Eq. 5)  
239 and  $f_{1 \rightarrow 2}(x_1, x_2)$  (Eq. 6) we treat compound one and two based on the difference  
240 in slopes in the conditional responses. Instead of speaking of the first and second  
241 compound, we speak of the smaller and larger one, referring to the order of  
242 steepness. Therefore, we use models Eq. 13 and Eq. 14, but categorize the  
243 compounds based on the slope parameter of their conditional response curves.  
244 This results in  $f_{\text{large} \rightarrow \text{small}}(x_1, x_2|\alpha)$  and  $f_{\text{small} \rightarrow \text{large}}(x_1, x_2|\alpha)$ .

245 Another synergy model we introduce here and refer to as  $f_{\text{geary}}(x_1, x_2|\alpha)$   
246 is based on a comment of Geary [2012], hence the naming. The two explicit

models  $f_{2 \rightarrow 1}(x_1, x_2)$  and  $f_{1 \rightarrow 2}(x_1, x_2)$  yield the same surface under the LACC but do rarely in practice. Therefore, it cannot be determined whether a response that lies between the two surfaces is synergistic or antagonistic and hence should be treated as non-interactive. Thus, if  $\alpha$  from  $f_{1 \rightarrow 2}(x_1, x_2|\alpha)$  and  $\alpha$  from  $f_{2 \rightarrow 1}(x_1, x_2|\alpha)$  are of equal sign, the synergy score of that model is computed as the mean of those two parameters. In case the two synergy parameters are of opposite sign, the synergy score is set to 0:

$$\alpha_{\text{geary}} = \begin{cases} \frac{1}{2}(\alpha_{1 \rightarrow 2} + \alpha_{2 \rightarrow 1}) & \text{if } \text{sign}(\alpha_{1 \rightarrow 2}) = \text{sign}(\alpha_{2 \rightarrow 1}) \\ 0 & \text{else} \end{cases}. \quad (16)$$

Next, to extend the null reference model following the principle of Bliss Independence, we extend Eq. 8 to

$$g_{\text{bliss}}(x_1, x_2|\alpha) = g_1(x_1) + g_2(x_2) - (1 + \alpha)g_1(x_1)g_2(x_2). \quad (17)$$

The motivation for this model is that any interaction between the two compounds is caught in the interaction term of the two conditional responses. In case of no interaction, the synergy parameter  $\alpha = 0$ , which leads to  $(1 + \alpha) = 1$ , and results in no deviance from the null reference model. As we use the formulation of Eq. 9 due to measuring the effect as survival, we reformulate Eq. 17 analogously as we did to get from Eq. 8 to Eq. 9: by replacing  $g_i(x_i)$  with  $1 - f_i(x_i)$ . Hence, Eq. 17 takes the form:

$$f_{\text{bliss}}(x_1, x_2|\alpha) = f_1(x_1)f_2(x_2) + \alpha(1 - f_1(x_1))(1 - f_2(x_2)) \quad (18)$$

This model does satisfy the requirement of no influence of the synergy parameter on conditional doses:  $f_{\text{bliss}}(x_1, 0|\alpha) = f_1(x_1)$  and  $f_{\text{bliss}}(0, x_2|\alpha) = f_2(x_2)$  as  $f_i(0) = 1$ . In case of synergy, the interactive effect is expected to be larger, therefore,  $\alpha$  being positive. If the compound combination has an antagonistic effect, the interaction term is expected to be smaller.

### 2.2.2 Lack-of-Fit Synergy

The second method to measure synergy investigated here is to compute the lack-of-fit of the measured response of a combination of compounds to the response of a null reference model derived from the conditional responses. We refer to this synergy value as  $\gamma$ :

$$\gamma = \int_{\min(x_2 > 0)}^{\max(x_2)} \int_{\min(x_1 > 0)}^{\max(x_1)} (\hat{y}(x_1, x_2|\Theta) - y(x_1, x_2)) d \log(x_1) d \log(x_2), \quad (19)$$

with  $\hat{y}(x_1, x_2|\Theta)$  the estimated effect with parameters  $\Theta$  of the fitted conditional responses following any non-interactive model and  $y$  the measured effect. Note that  $\hat{y}(\Theta)$  and  $y$  are dependent on the concentration combination  $(x_1, x_2)$ . This method was used in the AstraZeneca DREAM challenge [Menden et al., 2018] with the General Isobole Equation as null reference model and can be found in [Di Veroli et al., 2016]. Computing the volume has the advantage of taking the experimental design into account in contrast to simply taking the mean deviance over all measurement points, which is independent of the relative positions of the measurements. The degree of synergy varies for different dose



286 concentrations and transformations. The computed surface will be different for  
287 the same experiment if a log-transformation is applied to the doses or not.

288 In all, we have introduced six null reference models, five of them building  
289 up on the concept of Loewe Additivity and one on Bliss Independence. We  
290 further have introduced two methods to compute synergy, the parametric one  
291 and the lack-of-fit method. This results in twelve synergy model-method com-  
292 binations: the parametric ones,  $f_{\text{CI}}(x_1, x_2|\alpha)$  (Eq. 12),  $f_{\text{large}\rightarrow\text{small}}(x_1, x_2|\alpha)$   
293 and  $f_{\text{small}\rightarrow\text{large}}(x_1, x_2|\alpha)$  (Eq. 13, Eq. 14, dependent on the slope parameters)  
294 together with their mean,  $f_{\text{mean}}(x_1, x_2|\alpha)$  (Eq. 15), the method of Geary and  
295  $f_{\text{bliss}}(x_1, x_2|\alpha)$  (Eq. 17). For the lack-of-fit method, we take as the null refer-  
296 ence:  $f_{\text{CI}}(x_1, x_2)$  (Eq. 4),  $f_{\text{large}\rightarrow\text{small}}(x_1, x_2)$  and  $f_{\text{small}\rightarrow\text{large}}(x_1, x_2)$  (Eq. 5,  
297 Eq. 6), with the Explicit Mean Equation,  $f_{\text{mean}}(x_1, x_2)$  (Eq. 7), the method of  
298 Geary (analogously to Eq. 16) and  $f_{\text{bliss}}(x_1, x_2)$  (Eq. 9).

### 299 2.2.3 Fitting the Synergy Parameter

300 Before applying the two methods presented in Section 2.2.1 and Section 2.2.2,  
301 we normalize and clean the data from outliers. In a first step we normalize all  
302 records to the same value,  $y_0$ , the measured response at zero dose concentration  
303 from both compounds. Second, we discard outliers using the deviation from a  
304 spline approximation. Third, we fit both conditional responses of each record,  
305 namely the responses of each compound individually, to a pair of Hill curves  
306 (Eq. 21, Appendix A). We fit the response at zero dose concentration for both  
307 Hill curves. This gives the parameter set  $\Theta = \{y_0, y_{\infty,1}, y_{\infty,2}, e_1, e_2, s_1, s_2\}$  for  
308 each record. More details are given in Appendix B.

309 We apply the two different methods to calculate the synergy parameters  $\alpha$   
310 and  $\gamma$  to each record. First, for the parametrized synergy models, we apply a  
311 grid search for  $\alpha$ , for  $\alpha \in [-1, 1]$  with a step size of 0.01, minimizing the sum of  
312 squared errors. This gives the value of  $\alpha$  for which the squared error between  
313 the  $i^{\text{th}}$  measured effect  $y^{(i)}$  and  $i^{\text{th}}$  expected effect  $\hat{y}(x_1^{(i)}, x_2^{(i)}|\alpha, \Theta)$  is minimal:  
314

$$315 \min_{\alpha} \sum_{i=1, \text{ with } x_1^{(i)} \neq 0 \text{ and } x_2^{(i)} \neq 0}^N \left( \hat{y}(x_1^{(i)}, x_2^{(i)}|\alpha, \Theta) - y^{(i)} \right)^2. \quad (20)$$

316 Note that we exclude the conditional responses that we used to fit  $\Theta$  from the  
317 minimization. Second, we apply the lack-of-fit method from Di Veroli et al.  
318 [2016], where synergy is measured in terms of the integral difference in log  
319 space of measured response and surface spanned by the non-interactive models  
320 in Section 2.1, as given in Eq. 19. For the calculation of the integrals, we apply  
321 the trapezoidal rule [Press et al., 2007, Chapter 4].

## 322 2.3 Material

323 To evaluate the two methods introduced in Section 2.2.1 and Section 2.2.2, we  
324 apply them to two datasets of compound combination screening for which a  
325 categorization into the three synergy cases is provided.

326 The Mathews Griner dataset is a cancer compound synergy study by Mathews  
327 Griner et al. [2014]. In a one-to-all experimental design, the compound ibru-  
328 tinib was combined with 463 other compounds and administered to the cancer  
329 cell line TMD8 of which cell viability was measured. The dataset is published



at <https://tripod.nih.gov/matrix-client/>. Each compound combination was measured for 5 different doses, decreasing from  $125\mu M$  to  $2.5\mu M$  in a four-fold dilution for each compound alongside their conditional effects, resulting in 36 different dose combinations. The categorization of this dataset comes from a study by Yadav et al. [2015], in which every record was categorized based on a visual inspection.

The Cokol dataset comes from a study about fungal cell growth of the yeast *S. cerevisiae* (strain By4741), where Cokol et al. [2011] categorized the dataset. In this study the influence on cell growth was measured when exposed to 33 different compounds that were combined with one another based on promising combinations chosen by the authors, resulting in 200 different drug-drug-cell combinations. With an individually measured maximal effect dose for every compound, the doses administered decrease linearly in 7 steps with the eighth dose set to zero, resulting in an  $8 \times 8$  factorial design.

Based on the longest arc length of an isobole that is compared to the expected longest linear isobole in a non-interactive scenario, each record was given a score. In more detail, from the estimated surface of a record assuming no interaction, the longest contour line is measured in terms of its length and direction (convex or concave). A convex contour line leads to the categorization of a record as synergistic and the arc length of the longest contour line determines the strength of synergy. A concave contour line results in an antagonistic categorization with its extent being measured again as the length of the longest isobole. Thus the Cokol dataset not only comes with a classification but also with a synergy score similar to  $\alpha$  or  $\gamma$ .

To our knowledge, these two datasets are the only high-throughput ones with a classification into the three synergy classes: antagonistic, non-interactive and synergistic. Both datasets are somewhat imbalanced because interactions are rare [Borisy et al., 2003, Zhang et al., 2007, Farha and Brown, 2010]. The distribution of the classification is listed in Table 1. We obtained both categorizations after personal communication with the authors Yadav et al. [2015] and Cokol et al. [2011]. For the purpose of comparing the synergy models, we consider these two classifications as ground truth.

### 3 Results

Using the two methods of computing the synergy score, the parametric one (Section 2.2.1) and the lack-of-fit one (Section 2.2.2), we compute synergy scores for all records of the two datasets introduced in Section 2.3.

#### 3.1 Kendall rank correlation coefficient

Having obtained the synergy scores from the two different methods as described in Section 2.2.3, we compute the Kendall rank correlation coefficient, which is also known as Kendall's tau coefficient and was originally proposed by Kendall [1938]. This coefficient computes the rank correlation between the data as originally categorized by Yadav et al. [2015] and Cokol et al. [2011] and the computed synergy scores resulting from the two methods introduced in Section 2.2.1 and Section 2.2.2. For the analysis, we rank synergistic records highest at rank 3, followed by non-interactive at rank 2 and antagonistic lowest at rank 1. Due

375 to the many ties in rank, the Kendall rank correlation coefficient cannot take a  
376 value higher than 0.75 for Mathews Griner and 0.8 for Cokol, even if a perfect  
377 ranking was given. An overview of the Kendall rank correlation coefficients is  
378 given in Table 2 and Table 3 in Appendix C.

379 To compare parametric and lack-of-fit methods, we plot the correlation val-  
380 ues as a scatter plot per method (see Fig. 1) with the values from the parametric  
381 method plotted on the  $x$ -axis and those from the lack-of-fit method on the  $y$ -  
382 axis. Most of the points scatter in the upper left triangle, above the diagonal  
383 line. This shows that the lack-of-fit method outperforms the parametric method.  
384 This holds for all models applied to the Mathews Griner dataset and also for  
385 all models applied to the Cokol dataset. For both datasets, the highest cor-  
386 relation scores result from those null reference models that are based on the  
387 Loewe Additivity principle. The Bliss null reference model performs worst for  
388 the Mathews Griner set. For the Cokol data it is the second worst model. To a  
389 certain extent this can be explained as the classification of the Cokol dataset is  
390 based on isobole length relative to non-interactive, which is a Loewe Additivity  
391 type analysis. On both datasets the Explicit Mean Equation performs best with  
392 a correlation value of 0.55 and 0.62 for the Mathews Griner and Cokol dataset,  
393 respectively.

### 394 3.2 ROC-analysis

395 In high-throughput synergy studies, one generally screens for promising candi-  
396 dates that exhibit a synergistic or antagonistic effect. Those promising candi-  
397 dates are then investigated in more detail with genetic assays and other tech-  
398 niques. To determine how well the underlying null reference models result in  
399 distinguishable synergy scores, we conduct an ROC analysis (receiver operating  
400 characteristic), comparing the estimated synergy scores with the class categori-  
401 zation that is given for both datasets. A standard ROC analysis applies to  
402 binary classification, where cases are compared to controls. In this study, we  
403 have three classes: synergistic, antagonistic and non-interactive. We therefore  
404 compare each class to the combination of the other two, e.g. synergistic as cases  
405 versus the antagonistic and non-interactive combined as control. Typically, in  
406 ROC analyses, the cases rank higher than the controls. When treating the class  
407 antagonistic as case compared to the control synergistic and non-interactive we  
408 change all signs of the synergy scores. Therefore, the ranking of synergy scores  
409 is reversed and antagonistic synergy scores rank higher. Problems arise when  
410 comparing non-interactive cases to the control synergistic and antagonistic as  
411 their values should lie between the two control classes. Therefore, the absolute  
412 value of the estimated synergy scores is taken, which allows a ranking where  
413 the synergy scores of the non-interactive records should rank lower than the  
414 other synergy scores. Additionally, we can again multiply all synergy scores  
415 with minus one to revert the order of scores such that the cases rank higher.

416 The AUC values (area under the curve) are reported in Table 4 - Ta-  
417 ble 7 in Appendix C. For completeness, and based on the critique of Saito  
418 and Rehmsmeier [2015] to use PRC-AUC values for imbalanced datasets, the  
419 PRC-AUC values are also computed and can be found in Table 8 - Table 11 in  
420 Appendix C.

421 Analogously to the previous section, we depict the ROC values for both  
422 datasets in scatter plots (Fig. 2) with ROC values based on the parametric ap-

proach depicted on the  $x$ -axis and those based on the lack-of-fit approach on the  $y$ -axis. The underlying null reference models are shown by color. The different comparisons, such as synergistic versus non-interactive and antagonistic, are depicted by shape of the plot symbol. From Fig. 2, the dominance of the lack-of-fit approach over the parametric one is as apparent as from Fig. 1. With regard to the comparison of the different cases, visualized in shape, the ROC values from the comparison of the synergistic cases to the non-interactive and antagonistic controls, score the highest values around 0.9. The comparison of the non-interactive cases to the interactive ones score the lowest.

As the overall highest AUC scores result from the lack-of-fit method, we have a closer look at those for both datasets (Table 5 and Table 7 in Appendix C). For the antagonistic case, the values range around 0.80 for the Mathews Griner dataset and around 0.85 for the Cokol dataset. AUC values of the non-interactive case range around 0.75 for both datasets. The AUC values for the synergistic case for both datasets range around a value of 0.90 with one outlier of 0.77 for the Bliss Independence model on the Mathews Griner dataset.

Overall, the lack-of-fit outperforms the parametric method on both datasets. For the lack-of-fit method, the  $f_{\text{large} \rightarrow \text{small}}(x_1, x_2)$  performs best on the Mathews Griner dataset and is followed closely by the Explicit Mean Equation. On the second dataset, the Explicit Mean Equation performs overall best.

### 3.3 Scattering of Synergy Scores

To further investigate the performance of the methods and null reference models, we plot the synergy scores of the best performing models based on the Kendall rank correlation coefficient analysis (Section 3.1) and the ROC analysis (Section 3.2) for both datasets in Fig. 3, Fig. 4 and Fig. 5. In all figures, the overall correlation of the compared data is depicted together with the correlation per categorization. The coloring of the scores is based on the original categorization as antagonistic, non-interactive or synergistic as provided by Yadav et al. [2015] and Cokol et al. [2011].

In Fig. 3 the synergy scores computed with the lack-of-fit method are plotted against the original synergy scores from Cokol et al. [2011]. Applying the lack-of-fit method to the Bliss Independence model (Eq. 9) results in scores which are mainly above zero (Fig. 3, upper left). Further, it can be seen in the density plots along the  $y$ -axis in Fig. 3, upper left panel, and on the  $x$ -axis of Fig. 4, both panels in the first row and left panel in the middle row, that the synergy scores that are computed based on the principle of Bliss Independence cannot be easily separated by categorization, making it difficult to come up with a threshold to categorize a record into one of the three synergy categories (synergy, antagonism, non-interaction) given a synergy score.

For the other three models depicted in Fig. 3, that are based on the principle of Loewe Additivity, the synergy scores are more clearly separated. The computed scores of the synergistic records distribute nicely above zero in the upper right corner (categorized as synergistic and computed synergy scores above zero) as well as they scatter in the lower left corner for antagonistic cases. In all those three panels in Fig. 3 we see for the non-interactive records that the computed scores of those three models are both positive and negative ranging roughly between  $-0.1$  and  $0.1$  symmetrically. Barely any of the computed synergy scores for antagonistic cases are positive. Therefore, the chances of a record being

471 antagonistic if the synergy score is above zero are quite low as well as the risk  
472 of categorizing a record as antagonistic if it is synergistic.

473 We further looked in detail into dose combinations for which both the  $f_{GI}(x_1, x_2)$   
474 and  $f_{\text{mean}}(x_1, x_2)$  yield positive synergy values for antagonistic cases and into  
475 dose combinations for which the  $f_{\text{mean}}(x_1, x_2)$  model results in negative syn-  
476 ergy values for records which are labeled as synergistic. Those are all in all  
477 eight records. One of them is a compound combined with itself. Hence, per  
478 definition of the Loewe Additivity, no interaction is expected. We looked at  
479 the conditional responses of all eight dose combinations. At least one of the  
480 conditional responses exhibits small effects with the maximal response  $y_\infty$  be-  
481 ing above 0.65 (comp. left panel of Fig. 6). That leads to the computed null-  
482 reference surface to be quite high and hence causes synergistic scores if any  
483 effects are measured that are smaller than  $\max(y_\infty^{(1)}, y_\infty^{(2)})$ . We suspect that the  
484 dose concentrations are not well-sampled and larger maximal doses should have  
485 been administered.

486 We further looked up the seven dose combinations (excluding the one where  
487 the compound is combined with itself) in the Connectivity Map [Subramanian  
488 et al., 2017, Lamb et al., 2006]. Of those, we could find five in the Connectivity  
489 Map. All of these dose combinations showed non-interactive effects on all cell  
490 lines they were tested on. The assays found in the Connectivity Map are run  
491 on cancer cell lines. The dose combinations investigated here are run on yeast.  
492 Hence, a full comparison cannot be made.

493 In Fig. 4 and Fig. 5, the computed scores from different null reference mod-  
494 els are plotted against each other. We compare the implicit formulation (Gen-  
495 eral Isobole Equation) to the Bliss Independence model and the two best per-  
496 forming models that are based on the explicit formulation of Loewe Additivity,  
497  $f_{\text{mean}}(x_1, x_2)$  and  $f_{\text{large} \rightarrow \text{small}}(x_1, x_2)$ . The coloring of the scores is based on the  
498 original categorization as antagonistic, non-interactive or synergistic as provided  
499 by Yadav et al. [2015] and Cokol et al. [2011].

500 In Fig. 4 the scores from the Mathews Griner dataset are plotted. In the two  
501 panels in the upper row and the left panel in the middle row Bliss Independence  
502 is compared to the other three null models that build up on the principles of  
503 Loewe Additivity. The first three panels compare  $f_{\text{bliss}}(x_1, x_2)$  with the models  
504 based on the principle of Loewe Additivity. It is obvious, that the scores based  
505 on Bliss Independence are larger than those of Loewe Additivity and mainly  
506 above zero. The scores from models that are based on Loewe Additivity are  
507 very similar to each other, as they scatter along the diagonal (panels in middle  
508 right and lower row). It is difficult, though, to tell apart whether a record is  
509 synergistic or antagonistic, as non-interactive records scatter largely between  
510  $-0.5$  and  $0.5$ . Only records with a computed score outside that range can be  
511 categorized as interactive. For the Cokol dataset, which serves as basis for  
512 Fig. 5, the scores can be better separated. Despite the scores being generally  
513 smaller than those from the Mathews Griner data, the records can be easier  
514 separated, when using a Loewe Additivity based model. Additionally, we see  
515 here the similarity between these additive models given their strong correlation  
516 (right panels in middle row and both panels in lower row). Further, the scores  
517 based on  $f_{\text{large} \rightarrow \text{small}}(x_1, x_2)$  achieve higher values than those from the other  
518 two Loewe Additivity based models. This becomes obvious when comparing  
519 the null-reference surfaces of those three models, as depicted in [Lederer et al.,

2018, Fig. 4]. The surface spanned by  $f_{\text{large} \rightarrow \text{small}}(x_1, x_2)$  spans a surface above those surfaces spanned by Explicit Mean Equation or General Isobole Equation. Therefore, in synergistic cases where the measured effect is greater, and hence the response in cell death smaller, the difference from the null-reference surface to  $f_{\text{large} \rightarrow \text{small}}(x_1, x_2)$  is greater than to the other two models.

## 4 Discussion

The rise of high-throughput methods in recent years allows for massive screening of compound combinations. With the increase of data, there is an urge to develop methods that allow for reliable filtering of promising combinations. Further, the recent success of a synergy study of *in vivo* mice by Grüner et al. [2016] underlines the fast development of possibilities to generate biological data. Therefore, it is all the more important to develop methods that are sound and easily applicable to high-throughput data.

In this study we use two datasets of compound combinations that come with a categorization into synergistic, non-interactive or antagonistic for each record. Based on the fitted conditional responses, we compute the synergy scores of all records. We compare six models that build on the principles of Loewe Additivity and Bliss Independence. Those six models are used with two different methods to compute a synergy score for each record. The first method is a parametric approach and is motivated by the Combination Index introduced by Berenbaum [1977]. The second method quantifies the difference in volume between the expected response assuming no interaction and the measured response and is motivated by Di Veroli et al. [2016].

The computed synergy scores are compared in two different ways: first Kendall rank correlation coefficients are computed to investigate the reconstruction of ranking of the records (see Section 3.1), followed by an ROC analysis (Section 3.2) with the aim to verify the capacity, given a computed synergy score, to distinguish records from different categories. Both the Kendall rank correlation coefficient and the ROC analysis show a superiority of those models that are based on Loewe Additivity relative to those based on Bliss Independence. Note that we conduct the research only on combinations of two compounds. Meanwhile it is shown in Russ and Kishony [2018] that Bliss Independence maintains accuracy when increasing the number of compounds that are combined with each other while Loewe Additivity loses its predictive power for an increasing number of compounds. From those additive models the Explicit Mean Equation is the overall best performing model for both datasets. The comparison of the parametric method with the lack-of-fit method shows a superiority of the lack-of-fit method. To recall, the motivation behind the parametric approach was the statistical advantages of such an approach. It allows to define an interval around  $\alpha = 0$  in which a compound combination can be considered additive. For the lack-of-fit method, such statistical evaluation can not be done directly, but could be performed on the basis of bootstrapping.

Chou and Talalay [1977] measure the interaction effect locally for a fixed ratio of doses of both compounds that are supposed to reach the same effect, say one unit of the first compound causes the same effect as two units of the second compound, which results in the dose combination of 1:2. Along this fixed ratio of doses, they compute the left-hand side of Eq. 3 given the two doses  $x_1$  and  $x_2$

567 that are assumed to reach a fixed effect  $y^*$  together with  $x_i^*$  being the dose of  
568 compound  $i$  that reaches the fixed effect alone. For the fixed dose ratio, they run  
569 over all expected effects, usually from zero to one. A geometric interpretation  
570 of that method is depicted in [Greco et al., 1995, Fig. 7, p. 341]. The resulting  
571 values of the left-hand side of Eq. 3 are analyzed graphically: all computed values  
572 are plotted versus the expected fixed effect  $y^* = [0, 1]$ . Values higher than one  
573 exhibit synergistic behaviour, values below one antagonism. This method allows  
574 for results that show antagonistic behaviour for, say, smaller effects, as well as  
575 synergistic behaviour for higher effects, or vice versa. That such a behaviour of  
576 switching from antagonistic behaviour in one region to synergistic behaviour in  
577 another can occur was also shown in Norberg and Wahlström [1988]. Our main  
578 motivation in this study is to provide a single synergy score that allows for fast  
579 filtering of interesting candidates for more in-depth research. To extend that  
580 idea, standard deviation could further be taken into account. Additionally, the  
581 superior lack-of-fit method is much faster and simpler to implement than the  
582 parametric one.

583 Finally, to assess how distinguishable the synergy scores are, we visualize the  
584 synergy scores based on the underlying category (Section 3.3). The synergy  
585 scores from the lack-of-fit method can, based on their sign, reliably be catego-  
586 rized as synergistic or antagonistic. For records categorized as non-interactive,  
587 the computed synergy scores are positive as well as negative. For the two  
588 datasets, we saw different extents of separation between those scores, which  
589 makes it difficult to generalize the results. All in all, the differentiation from no  
590 interaction poses a more difficult task as choosing the threshold is arbitrary.

591 For Bliss Independence such a differentiation is barely possible due to a  
592 strong overlap of synergy scores from all three categories and mainly positive  
593 synergy scores from the lack-of-fit method. Different ranges of synergy scores  
594 for both datasets make it additionally difficult to assess synergy or antagonism  
595 for a record based on the unique information of the synergy score.

596 Finally, we want to emphasize the performance benefit of the recently intro-  
597 duced Explicit Mean Equation [Lederer et al., 2018] over the implicit formulation  
598 in form of the General Isobole Equation. The explicit formulation of this addi-  
599 tive model does not only show higher accuracy in prediction performance but  
600 was also shown to speed up computation by a factor of 250. Although the per-  
601 formance of models and method are consistent across the two (quite different)  
602 datasets considered in this study, reliable comparison of different methods would  
603 benefit from the availability of more ground truth drug screening datasets.



## Acknowledgments

604

We thank Bhagwan Yadav for the sharing of the code used for the analysis in Yadav et al. [2015] and Murat Cokol for the sharing of the data and analytical insights from Cokol et al. [2011].

605

606

607

## Conflict of Interest

608

The authors declare that they have no conflict of interest.

609

## Funding

610

This work was supported by the Radboud University and CogIMon H2020 ICT-644727.

611

612

## References

613

S Loewe. Die quantitativen Probleme der Pharmakologie. *Ergebnisse der Physiologie*, 27(1):47–187, 1928. ISSN 03034240. doi: 10.1007/BF02322290.

614

615

C I Bliss. The toxicity of poisons applied jointly. *Ann. Appl. Biol.*, 26(3):585–615, 1939. ISSN 00034746. doi: 10.1111/j.1744-7348.1939.tb06990.x.

616

617

Simone Lederer, Tjeerd M H Dijkstra, and Tom Heskes. Additive Dose Response Models: Explicit Formulation and the Loewe Additivity Consistency Condition. *Front. Pharmacol.*, 9(February):1–11, 2018. doi: 10.3389/fphar.2018.00031. URL <https://www.frontiersin.org/articles/10.3389/fphar.2018.00031/full>.

618

619

620

621

622

Bhagwan Yadav, Krister Wennerberg, Tero Aittokallio, and Jing Tang. Searching for Drug Synergy in Complex Dose-Response Landscapes Using an Interaction Potency Model. *Comput. Struct. Biotechnol. J.*, 13:504–513, 2015. ISSN 20010370. doi: 10.1016/j.csbj.2015.09.001. URL <http://dx.doi.org/10.1016/j.csbj.2015.09.001>.

623

624

625

626

627

Murat Cokol, Hon Nian Chua, Murat Tasan, Beste Mutlu, Zohar B Weinstein, Yo Suzuki, Mehmet E Nergiz, Michael Costanzo, Anastasia Baryshnikova, Guri Giaever, Corey Nislow, Chad L Myers, Brenda J Andrews, Charles Boone, and Frederick P Roth. Systematic exploration of synergistic drug pairs. *Mol. Syst. Biol.*, 7(544), 2011. ISSN 1744-4292. doi: 10.1038/msb.2011.71.

628

629

630

631

632

633

William R Greco, Gergory Bravo, and John C Parsons. The Search for Synergy: A Critical Review from A Response Surface Perspective. *Pharmacol. Rev.*, 47(2):331–385, 1995.

634

635

636

Nori Geary. Understanding Synergy. *Am. J. Physiol. Endocrinol. Metab.*, 304(3):E237–E253, 2012. ISSN 1522-1555. doi: 10.1152/ajpendo.00308.2012. URL <http://www.ncbi.nlm.nih.gov/pubmed/23211518>.

637

638

639



- 640 Charles F Minto, Thomas W Schnider, Timothy G Short, Keith M Gregg, An-  
641 drea Gentilini, and Steven L Shafer. Response Surface Model for Anesthetic  
642 Drug Interactions. *Anesthesiology*, 92(6):1603–1606, 2000.
- 643 Ting-Chao Chou and Paul Talalay. Quantitative analysis of dose-effect rela-  
644 tionships: the combined effects of multiple drugs or enzyme inhibitors. *Adv.*  
645 *Enzyme Regul.*, 22:27–55, 1984. doi: 10.1016/0065-2571(84)90007-4.
- 646 Giovanni Y Di Veroli, Chiara Fornari, Dennis Wang, Severine Mollard,  
647 Jo L Bramhall, Frances M Richards, and Duncan I Jodrell. Comben-  
648 efit: An interactive platform for the analysis and visualisation of drug  
649 combinations. *Bioinformatics*, 32(18):2866–2868, 2016. ISSN 1367-4803.  
650 doi: 10.1093/bioinformatics/btw230. URL [http://bioinformatics.](http://bioinformatics.oxfordjournals.org/content/early/2016/05/27/bioinformatics.btw230.full.pdf%7D5Cnhttp://bioinformatics.oxfordjournals.org/content/early/2016/04/25/bioinformatics.btw230.abstract)  
651 [oxfordjournals.org/content/early/2016/05/27/bioinformatics.](http://bioinformatics.oxfordjournals.org/content/early/2016/05/27/bioinformatics.btw230.full.pdf%7D5Cnhttp://bioinformatics.oxfordjournals.org/content/early/2016/04/25/bioinformatics.btw230.abstract)  
652 [btw230.full.pdf%7D5Cnhttp://bioinformatics.oxfordjournals.org/](http://bioinformatics.oxfordjournals.org/content/early/2016/04/25/bioinformatics.btw230.abstract)  
653 [content/early/2016/04/25/bioinformatics.btw230.abstract](http://bioinformatics.oxfordjournals.org/content/early/2016/04/25/bioinformatics.btw230.abstract).
- 654 Powerful combination therapies. *Nat. Biomed. Eng.*, 2(8):555–556, 2018. ISSN  
655 2157-846X. doi: 10.1038/s41551-018-0283-1. URL [https://doi.org/10.](https://doi.org/10.1038/s41551-018-0283-1)  
656 [1038/s41551-018-0283-1](https://doi.org/10.1038/s41551-018-0283-1).
- 657 Joseph Lehar, Grant R Zimmermann, Andrew S Krueger, Raymond A Mol-  
658 nar, Jebediah T Ledell, Adrian M Heilbut, Glenn F Short, Leanne C Giusti,  
659 Garry P Nolan, Omar A Magid, Margaret S Lee, Alexis A Borisy, Brent R  
660 Stockwell, and Curtis T Keith. Chemical combination effects predict connec-  
661 tivity in biological systems. *Mol. Syst. Biol.*, 3(80):80, 2007. ISSN 1744-4292.  
662 doi: 10.1038/msb4100116.
- 663 Ting-Chao Chou and Paul Talalay. A Simple Generalized Equation for the  
664 Analysis of Multiple Inhibitions of Michaelis-Menten Kinetic Systems. *J.*  
665 *Biol. Chem.*, 252(18):6438–6442, 1977.
- 666 M.C. Berenbaum. Synergy, additivism and antagonism in immunosuppression.  
667 *Clin. exp. Immunol.*, 28:1–18, 1977.
- 668 Michael Patrick Menden, Dennis Wang, Yuanfang Guan, Michael Mason, Bence  
669 Szalai, Krishna C Bulusu, Thomas Yu, Jaewoo Kang, Minji Jeon, Russ  
670 Wolfinger, Tin Nguyen, Mikhail Zaslavskiy, In Sock Jang, Zara Ghazoui,  
671 Mehmet Eren Ahsen, Robert Vogel, Elias Chaibub Neto, Thea Norman, Eric  
672 K Y Tang, Mathew J Garnett, Giovanni Di Veroli, Stephen Fawell, Gustavo  
673 Stolovitzky, Justin Guinney, Jonathan R Dry, and Julio Saez-Rodriguez. A  
674 cancer pharmacogenomic screen powering crowd-sourced advancement of drug  
675 combination prediction. *bioRxiv*, 2018. URL [http://biorxiv.org/content/](http://biorxiv.org/content/early/2018/02/13/200451.abstract)  
676 [early/2018/02/13/200451.abstract](http://biorxiv.org/content/early/2018/02/13/200451.abstract).
- 677 William H Press, Saul A Teukolsky, William T Vetterling, and Brian P Flannery.  
678 *Numerical Recipes: The Art of Scientific Computing*, volume 1. Cambridge  
679 University Press, Cambridge, 3 edition, 2007. ISBN 0521880688. doi: 10.  
680 1137/1031025.
- 681 Lesley A Mathews Griner, Rajarshi Guha, Paul Shinn, Ryan M Young,  
682 Jonathan M Keller, Dongbo Liu, Ian S Goldlust, Adam Yasgar, Crystal McK-  
683 night, Matthew B Boxer, Damien Y Duveau, Jian-Kang Jiang, Sam Michael,

- Tim Mierzwa, Wenwei Huang, Martin J Walsh, Bryan T Mott, Paresma Patel, William Leister, David J Maloney, Christopher A Leclair, Ganesha Rai, Ajit Jadhav, Brian D Peyser, Christopher P Austin, Scott E Martin, Anton Simonov, Marc Ferrer, Louis M Staudt, and Craig J Thomas. High-throughput combinatorial screening identifies drugs that cooperate with ibrutinib to kill activated B-cell-like diffuse large B-cell lymphoma cells. *Proc. Natl. Acad. Sci. U. S. A.*, 111(6):2349–54, 2014. ISSN 1091-6490. doi: 10.1073/pnas.1311846111. URL <http://www.pnas.org/cgi/content/long/111/6/2349>.
- Alexis A Borisy, Peter J Elliott, Nicole W Hurst, Margaret S Lee, Joseph Lehar, E Roydon Price, George Serbedzija, Grant R Zimmermann, Michael A Foley, Brent R Stockwell, and Curtis T Keith. Systematic discovery of multicomponent therapeutics. *Proc. Natl. Acad. Sci. U. S. A.*, 100(13):7977–7982, 2003. ISSN 0027-8424. doi: 10.1073/pnas.1337088100.
- L Zhang, K Yan, Y Zhang, R Huang, J Bian, C Zheng, H Sun, Z Chen, N Sun, R An, F Min, W Zhao, Y Zhuo, J You, Y Song, Z Yu, Z Liu, K Yang, H Gao, H Dai, X Zhang, J Wang, C Fu, G Pei, J Liu, S Zhang, M Goodfellow, Y Jiang, J Kuai, G Zhou, and X Chen. High-throughput synergy screening identifies microbial metabolites as combination agents for the treatment of fungal infections. *Proc. Natl. Acad. Sci. U. S. A.*, 104(11):4606–4611, 2007. ISSN 0027-8424. doi: 10.1073/pnas.0609370104. URL <http://www.ncbi.nlm.nih.gov/pubmed/17360571>.
- Maya A Farha and Eric D Brown. Chemical probes of escherichia coli uncovered through chemical-chemical interaction profiling with compounds of known biological activity. *Chem. Biol.*, 17(8):852–862, 2010. ISSN 10745521. doi: 10.1016/j.chembiol.2010.06.008. URL <http://dx.doi.org/10.1016/j.chembiol.2010.06.008>.
- M G Kendall. A new Measure of Rank Correlation. *Biometrika*, 30(1-2):81–93, 1938. doi: 10.1093/biomet/30.1-2.81. URL <http://dx.doi.org/10.1093/biomet/30.1-2.81>.
- Takaya Saito and Marc Rehmsmeier. The precision-recall plot is more informative than the ROC plot when evaluating binary classifiers on imbalanced datasets. *PLoS One*, 10(3):1–21, 2015. ISSN 19326203. doi: 10.1371/journal.pone.0118432.
- Aravind Subramanian, Rajiv Narayan, Steven M Corsello, David D Peck, Ted E Natoli, Xiaodong Lu, Joshua Gould, John F Davis, Andrew A Tubelli, Jacob K Asiedu, David L Lahr, Jodi E Hirschman, Zihan Liu, Melanie Donahue, Bina Julian, Mariya Khan, David Wadden, Ian C Smith, Daniel Lam, Arthur Liberzon, Courtney Toder, Mukta Bagul, Marek Orzechowski, Oana M Enache, Federica Piccioni, Sarah A Johnson, Nicholas J Lyons, Alice H Berger, Alykhan F Shamji, Angela N Brooks, Anita Vrcic, Corey Flynn, Jacqueline Rosains, David Y Takeda, Roger Hu, Desiree Davison, Justin Lamb, Kristin Ardlie, Larson Hogstrom, Peyton Greenside, Nathanael S Gray, Paul A Clemons, Serena Silver, Xiaoyun Wu, Wen Ning Zhao, Willis Read-Button, Xiaohua Wu, Stephen J Haggarty, Lucienne V Ronco, Jesse S Boehm, Stuart L Schreiber, John G Doench, Joshua A Bittker, David E

- 729 Root, Bang Wong, and Todd R Golub. A Next Generation Connectivity  
730 Map: L1000 Platform and the First 1,000,000 Profiles. *Cell*, 171(6):  
731 1437–1452.e17, 2017. ISSN 10974172. doi: 10.1016/j.cell.2017.10.049. URL  
732 <http://dx.doi.org/10.1016/j.cell.2017.10.049>.
- 733 Justin Lamb, Emily D Crawford, David Peck, Joshua W Modell, Irene C Blat,  
734 Matthew J Wrobel, Jim Lerner, Jean-Philippe Brunet, Aravind Subramanian,  
735 Kenneth N Ross, Michael Reich, Haley Hieronymus, Guo Wei, Scott A Arm-  
736 strong, Stephen J Haggarty, Paul A Clemons, Ru Wei, and Steven A Carr.  
737 The Connectivity Map : Using Gene-Expression Signatures to Connect Small  
738 Molecules, Genes, and Disease. *Science (80-. )*, 313(September):1929–1935,  
739 2006. ISSN 1095-9203. doi: 10.1126/science.1132939.
- 740 Barbara M Grüner, Christopher J Schulze, Dian Yang, Daisuke Ogasawara,  
741 Melissa M Dix, Zoë N Rogers, Chen-Hua Chuang, Christopher D McFarland,  
742 Shin-Heng Chiou, J Mark Brown, Benjamin F Cravatt, Matthew Bogoy, and  
743 Monte M Winslow. An in vivo multiplexed small-molecule screening platform.  
744 *Nat. Methods*, 13(September), 2016. ISSN 1548-7091. doi: 10.1038/nmeth.  
745 3992. URL <http://www.nature.com/doi/10.1038/nmeth.3992>.
- 746 D Russ and R Kishony. Additivity of inhibitory effects in mul-  
747 tidrug combinations. *Nat. Microbiol.*, 2018. ISSN 2058-5276.  
748 doi: 10.1038/s41564-018-0252-1. URL <http://dx.doi.org/10.1038/s41564-018-0252-1>.
- 750 L Norberg and G Wahlström. Anaesthetic effects of flurazepam alone and  
751 in combination with thiopental or hexobarbital evaluated with an EEG-  
752 threshold method in male rats. *Arch. Int. des Pharmacodyn. Ther.*, (292):  
753 45–57, 1988.
- 754 A V Hill. The possible effects of the aggregation of the molecule of hemoglobin  
755 on its dissociation curves. *J. Physiol.*, 40:iv–vii, 1910.
- 756 Sylvain Goutelle, Michel Maurin, Florent Rougier, Xavier Barbaut, Laurent  
757 Bourguignon, Michel Ducher, and Pascal Maire. The Hill equation: A review  
758 of its capabilities in pharmacological modelling. *Fundam. Clin. Pharmacol.*,  
759 22(6):633–648, 2008. ISSN 07673981. doi: 10.1111/j.1472-8206.2008.00633.x.
- 760 Christian Ritz and Jens C Streibig. *drc: Analysis of Dose-Response Curves*,  
761 2016. URL <https://cran.r-project.org/package=drc>.
- 762 Simon Wood. *Generalized Additive Models: an introduction with R*. Chapman  
763 and Hall/CRC, 2 edition, 2017. ISBN 1584884746. doi: 10.1111/j.1541-0420.  
764 2006.00574.x.
- 765 Simon N Wood. Fast stable restricted maximum likelihood and marginal likeli-  
766 hood estimation of semiparametric generalized linear models. *J. R. Stat. Soc.*,  
767 73(1):3–36, 2011. ISSN 13697412. doi: 10.1111/j.1467-9868.2010.00749.x.
- 768 Christian Ritz, Florent Baty, Jens C Streibig, and Daniel Gerhard. Dose-  
769 response analysis using R. *PLoS One*, 10(12):1–13, 2015. ISSN 19326203. doi:  
770 10.1371/journal.pone.0146021. URL [http://journals.plos.org/plosone/  
771 article?id=10.1371/journal.pone.0146021](http://journals.plos.org/plosone/article?id=10.1371/journal.pone.0146021).

R Core Team. *R: A Language and Environment for Statistical Computing*. R 772  
Foundation for Statistical Computing, Vienna, Austria, 2016. URL [https:](https://www.r-project.org/) 773  
[//www.r-project.org/](https://www.r-project.org/). 774

## 775 Tables

	synergistic	antagonistic	non-interactive
Mathews Griner	121	90	252
Cokol	50	68	82

Table 1: Number of cases categorized as synergistic, antagonistic or non-interactive in the two datasets Mathews Griner and Cokol.

## Figure Captions

776

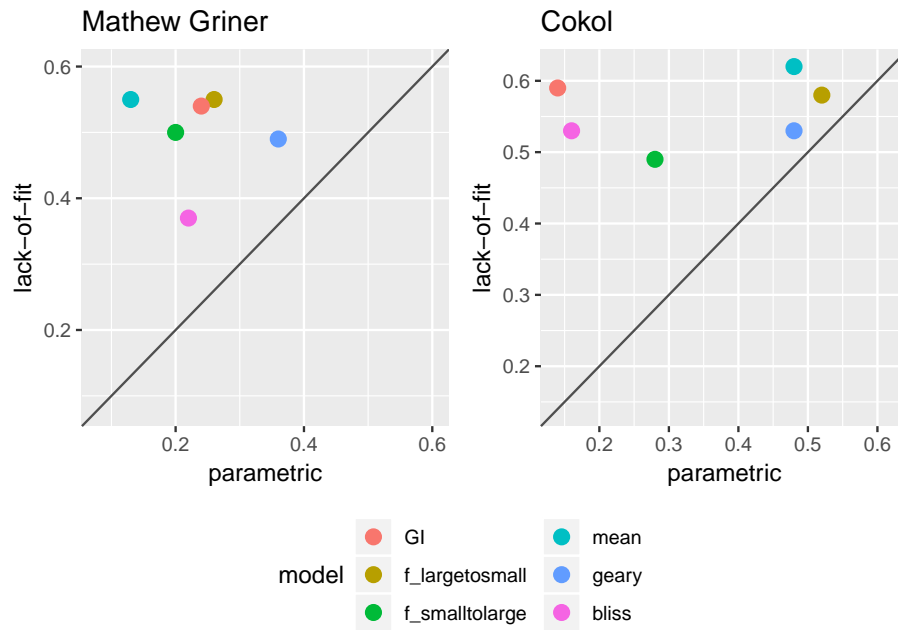


Figure 1: Scatter plot of Kendall rank correlation coefficient for both datasets, Mathews Griner (left) and Cokol (right). The correlation values resulting from the parametric approach are plotted on the  $x$ -axis and those from the lack-of-fit approach are plotted on the  $y$ -axis. To guide the eye, the diagonal is plotted.

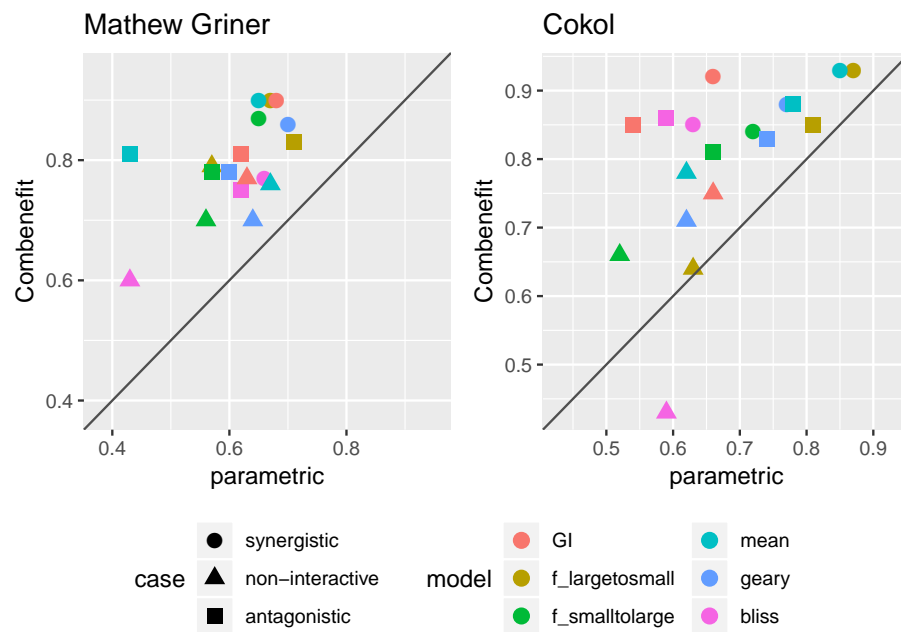


Figure 2: Scatter plot of ROC values for both datasets, Mathews Griner (left) and Cokol (right). The ROC values resulting from the parametric approach are plotted on the  $x$ -axis and those from the lack-of-fit approach are plotted on the  $y$ -axis. To guide the eye, the diagonal is plotted. The three different comparisons, of one case versus the remaining two, are depicted in different shapes.



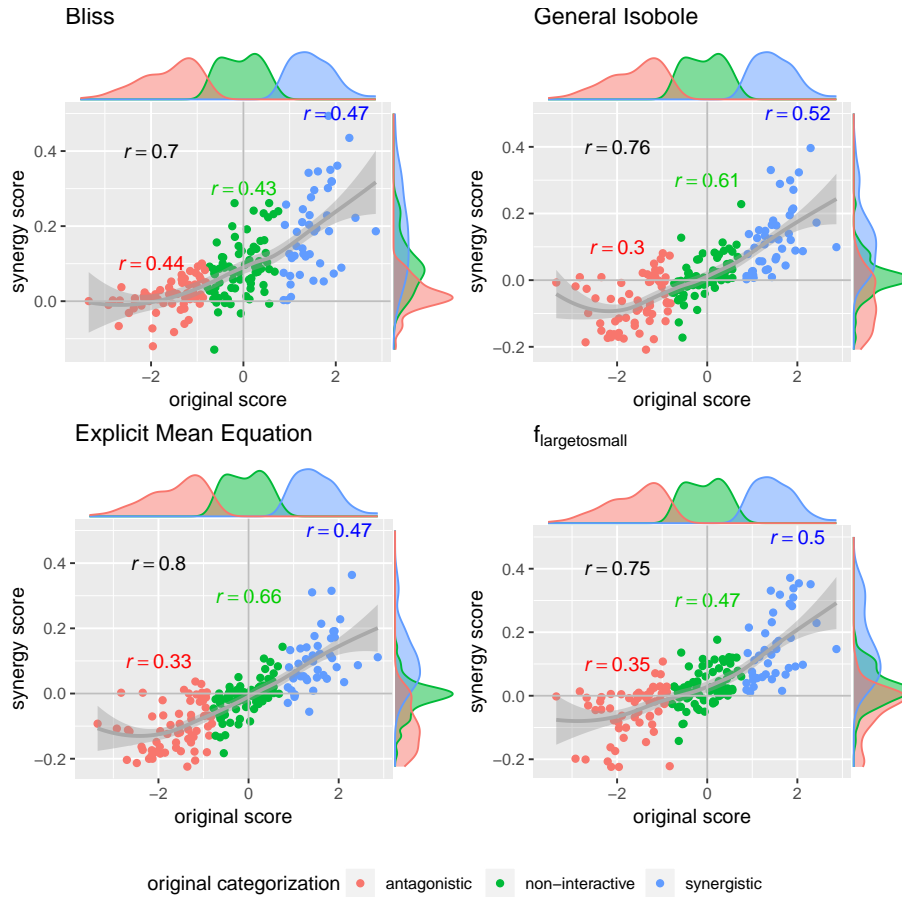


Figure 3: Computed synergy scores of Cokol data of best methods according to the Kendall rank correlation coefficient and ROC analysis in Section 3.1 and Section 3.2 in comparison to the original scores from Cokol et al. [2011]. Further, for all three categories, synergistic, non-interactive and antagonistic, the Pearson correlation is depicted between the original scores in that category and the computed synergy scores. The correlation value for each category is depicted above every class. Additionally, we depict the local polynomial regression fitting of all scores (in gray). Furthermore, the histograms of the scores are plotted on the axis, separated by color based on the original categorization.

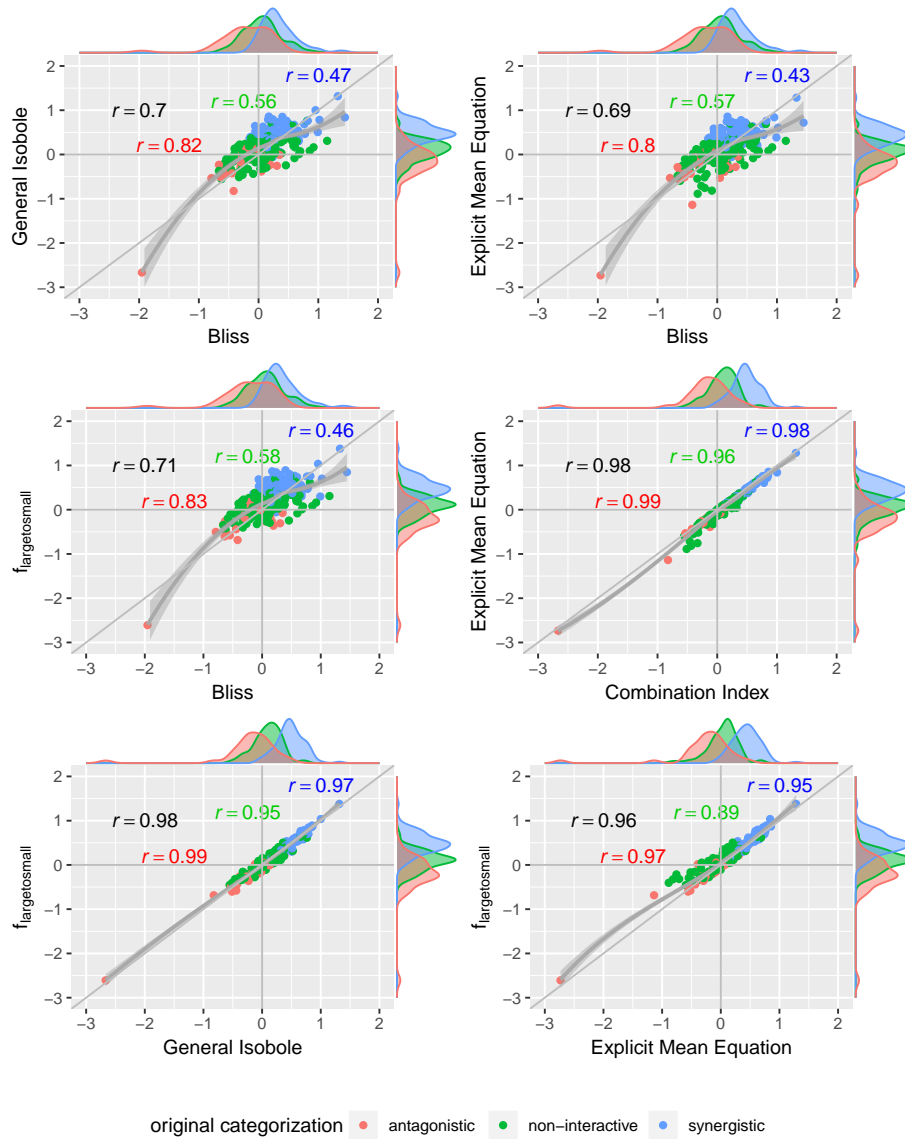


Figure 4: Computed synergy scores of Mathews Griner data computed with the lack-of-fit method. Displayed are the four best models according to the Kendall rank correlation coefficient and ROC analysis in Section 3.1 and Section 3.2, the scores of one model on the  $x$ -axis and the other on the  $y$ -axis.

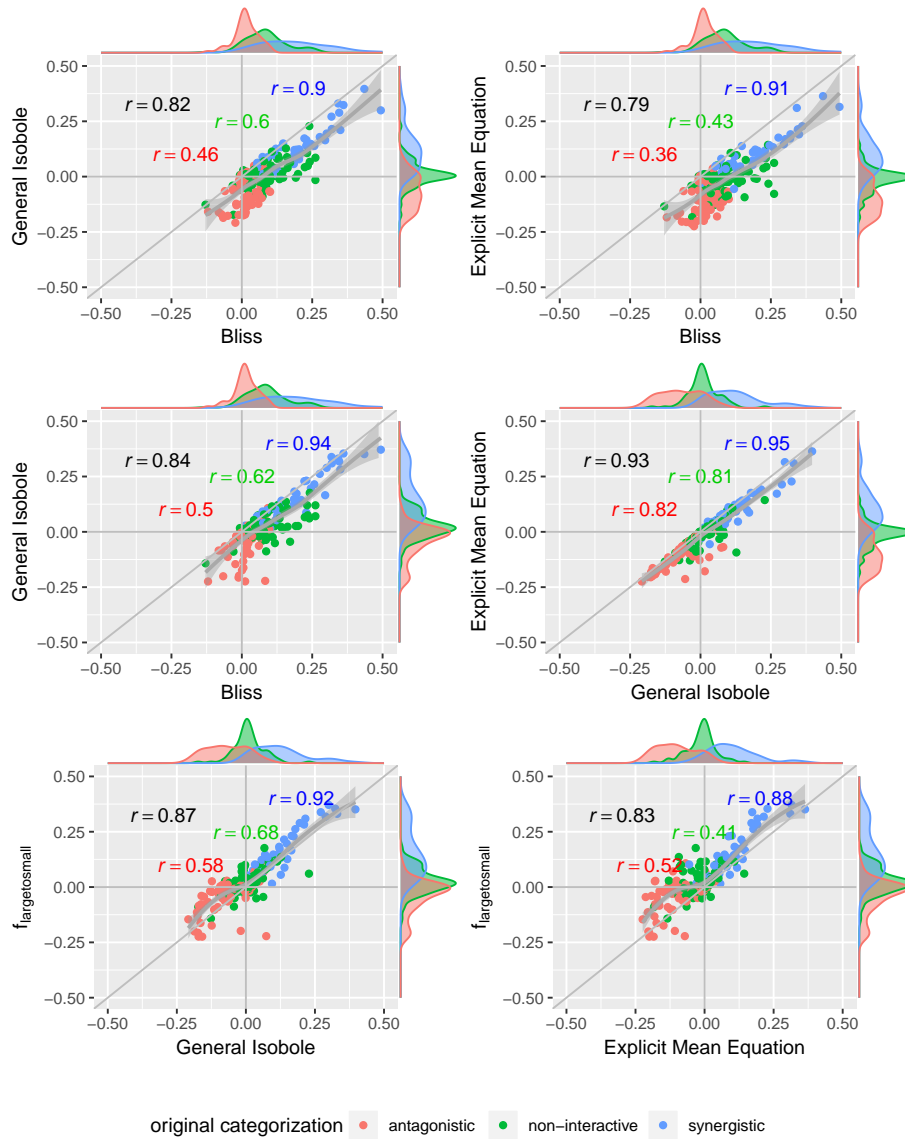


Figure 5: Computed synergy scores of Cokol data computed with the lack-of-fit method. Displayed are the four best models according to the Kendall rank correlation coefficient and ROC analysis in Section 3.1 and Section 3.2, the scores of one model on the  $x$ -axis and the other on the  $y$ -axis.

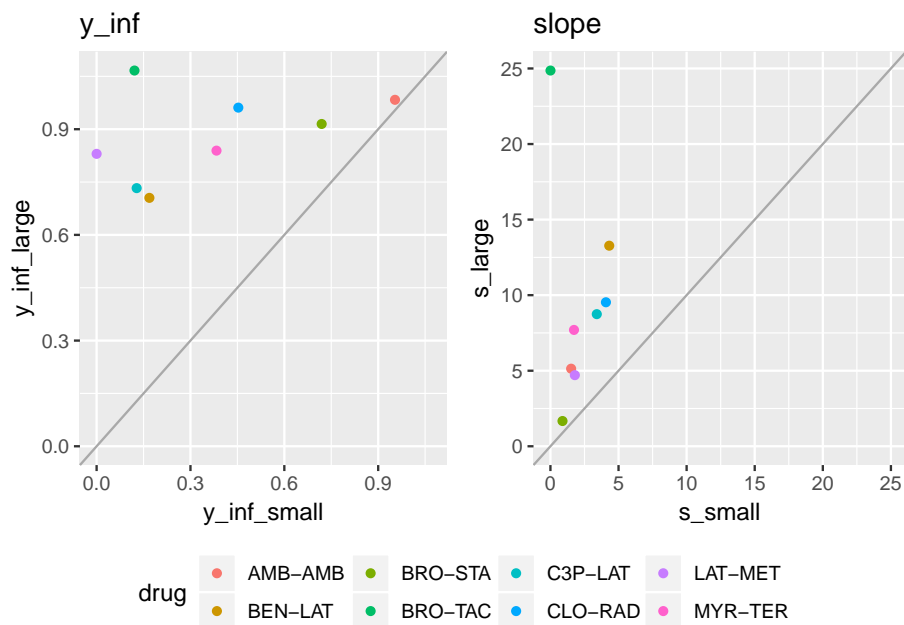


Figure 6: Maximal response (left) and slope parameters (right) of the conditional responses of the eight cases for which the lack-of-fit method resulted for  $f_{\text{mean}}(x_1, x_2)$  and  $f_{\text{GI}}(x_1, x_2)$  in a synergy score of opposite sign to its categorization.

## A Conditional Dose Response Curves

777

A common approach for modeling monotonic dose-response curves  $f_j$  with  $j \in \{1, 2\}$  is the Hill curve [Hill, 1910], also referred to as the sigmoid function. The Hill model is, due to its good fit to many sources of data, the most widely applied model for fitting compound responses [Goutelle et al., 2008]. It has a sigmoidal shape with little change for small doses but with a rapid decline in response once a certain threshold is met. For even larger doses the effect asymptotes to a constant maximal effect. Two exemplary Hill curves are depicted in Fig. 7. There are several parameterizations of the Hill curve. We use the following

778

779

780

781

782

783

784

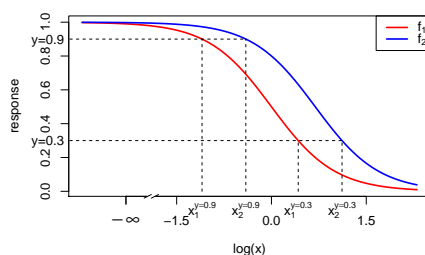


Figure 7: Dose-response curves (red and blue) as Hill curves (Eq. 21). For the exemplary responses of 0.3 and 0.9 the different doses  $x_1$  and  $x_2$  reaching that effect are shown (dashed lines). The dose-response curves differ only in  $EC_{50}$  with  $e_1 = 2$  and  $e_2 = 1$ . Values of the other parameters are  $y_0 = 1$ ,  $y_\infty = 0$  and  $s = 2$ . To highlight the sigmoidal shape of a Hill curve in log-space, the logarithmic concentration space is depicted.

785

786

throughout this study to fit conditional responses:

$$f(x) = y_\infty + \frac{y_0 - y_\infty}{1 + \left(\frac{x}{e}\right)^s}, \quad (21)$$

787

where  $y_0$  is the response at zero dose and  $y_\infty$  the maximal response of the cells to the compound,  $e$  the dose concentration reaching half of the maximal response and  $s$  the steepness of the curve. Eq. 21 is equivalent to the parametrization used in the drc package [Ritz and Strebig, 2016], the so-called four parameter log-logistic model. By our definition of the Hill curve, a positive  $s$  leads to a descending Hill curve.

788

789

790

791

792

793

## 794 **B Data Cleaning, Fitting of Hill Curve and Pa-** 795 **rameter Estimation for Implicit Models**

796 First, we normalize all records by the measured response at zero dose concen-  
797 tration from both compounds,  $y_0$ . Second, we conduct an outlier analysis of the  
798 normalized responses by fitting a spline surface and deleting outliers to discard  
799 them. Third, we then fit the conditional responses of the cleaned data to Hill  
800 curves.

801 We fit a general additive model (GAM) to the normalized raw data using thin  
802 plate splines [Wood, 2017], not transforming the doses in any way. The surfaces  
803 of those fitted thin plate splines span the checkerboards of every record and  
804 data points with too large absolute residual values are rejected. For fitting the  
805 splines we use method `gam()` of the `mgcv`-package [Wood, 2011]. The threshold  
806 to reject data points is at three times the inter-quantile range of all residuals of  
807 a given record. Every data point with an absolute residual above that threshold  
808 is discarded. For the Mathews Griner data, this leads to 125 records out of  
809 the 466 (less than 30%) where a mean of 1.59 outliers were excluded per record  
810 with an overall of 199 data points excluded, which is less than one percent of  
811 the overall data. A maximum of 6 outliers was detected once. Similarly, we  
812 excluded on average 4.21 data points for the Cokol data on 150 of the total 200  
813 (75%) records with a maximum of 13 data points and an overall of 623 data  
814 points excluded, which is about 8.7% of all data points.

815 To fit the two conditional responses of a record to two Hill functions of the  
816 form of Eq. 21 we use the `drc` package [Ritz et al., 2015]. Unlike other synergy  
817 analyses such as [Yadav et al., 2015], the response at zero concentration  $y_0$  is not  
818 fixed to 1 but merely constrained to be the same for both response curves. The  
819 other Hill parameters,  $y_\infty$ ,  $s$  and  $e$  are fitted for both compounds individually.  
820 In case the asymptote parameter  $y_\infty$  is below zero for any of the two Hill curves,  
821 the conditional response of that compound is refitted to a two-parameter model  
822 with  $y_\infty$  set to zero and  $y_0$  kept from the fitting of both compounds together.  
823 This is the case for 43 records of the Mathews Griner dataset and 125 records  
824 of the Cokol dataset.

825 The  $f_{GI}(x_1, x_2)$  model is an implicit model for the response  $y$ . Therefore,  
826 a root finder is used to find a response  $\hat{y}^{(i)}$  given concentrations  $(x_1^{(i)}, x_2^{(i)})$   
827 and parameters describing the Hill curves of the conditional responses,  $\Theta =$   
828  $\{y_0, y_{\infty, j}, e_j, s_j\}$ . We used the standard implementation of a root finder in the  
829 R stats package, `uniroot()` [R Core Team, 2016], which is based on the Brent-  
830 Dekker-van Wijngaarden algorithm [Press et al., 2007, Chapter 9]. As conver-  
831 gence criterion we used  $1.22 \times 10^{-4}$ .

## C Supplementary Tables

832

model	lack-of-fit	parametric
$f_{\text{GI}}(x_1, x_2)$	0.54	0.24
$f_{\text{large} \rightarrow \text{small}}(x_1, x_2)$	0.55	0.26
$f_{\text{small} \rightarrow \text{large}}(x_1, x_2)$	0.50	0.20
$f_{\text{mean}}(x_1, x_2)$	<b>0.55</b>	0.13
$f_{\text{geary}}(x_1, x_2)$	0.49	<b>0.36</b>
$f_{\text{bliss}}(x_1, x_2)$	0.37	0.22

Table 2: Kendall rank correlation coefficient of Mathews Griner dataset.

model	lack-of-fit	parametric
$f_{\text{GI}}(x_1, x_2)$	0.59	0.14
$f_{\text{large} \rightarrow \text{small}}(x_1, x_2)$	0.58	<b>0.52</b>
$f_{\text{small} \rightarrow \text{large}}(x_1, x_2)$	0.49	0.28
$f_{\text{mean}}(x_1, x_2)$	<b>0.62</b>	0.48
$f_{\text{geary}}(x_1, x_2)$	0.53	0.48
$f_{\text{bliss}}(x_1, x_2)$	0.53	0.16

Table 3: Kendall rank correlation coefficient of Cokol dataset.

	synergistic	non-interactive	antagonistic
$f_{\text{GI}}(x_1, x_2)$	0.68	0.63	0.62
$f_{\text{large} \rightarrow \text{small}}(x_1, x_2)$	0.67	0.57	<b>0.71</b>
$f_{\text{small} \rightarrow \text{large}}(x_1, x_2)$	0.65	0.56	0.57
$f_{\text{mean}}(x_1, x_2)$	0.65	<b>0.67</b>	0.43
$f_{\text{geary}}(x_1, x_2)$	<b>0.70</b>	0.64	0.60
$f_{\text{bliss}}(x_1, x_2)$	0.66	0.43	0.62

Table 4: AUC analysis of parametric method applied to Mathews Griner dataset.



	synergistic	non-interactive	antagonistic
$f_{GI}(x_1, x_2)$	<b>0.90</b>	0.77	0.81
$f_{large \rightarrow small}(x_1, x_2)$	<b>0.90</b>	<b>0.79</b>	<b>0.83</b>
$f_{small \rightarrow large}(x_1, x_2)$	0.87	0.70	0.78
$f_{mean}(x_1, x_2)$	<b>0.90</b>	0.76	0.81
$f_{geary}(x_1, x_2)$	0.86	0.70	0.78
$f_{bliss}(x_1, x_2)$	0.77	0.60	0.75

Table 5: AUC analysis on lack-of-fit method applied to Mathews Griner dataset.

	synergistic	non-interactive	antagonistic
$f_{GI}(x_1, x_2)$	0.66	<b>0.66</b>	0.54
$f_{large \rightarrow small}(x_1, x_2)$	<b>0.87</b>	0.63	<b>0.81</b>
$f_{small \rightarrow large}(x_1, x_2)$	0.72	0.52	0.66
$f_{mean}(x_1, x_2)$	0.85	0.62	0.78
$f_{geary}(x_1, x_2)$	0.77	0.62	0.74
$f_{bliss}(x_1, x_2)$	0.63	0.59	0.59

Table 6: AUC analysis on parametric method applied to Cokol dataset.

	synergistic	non-interactive	antagonistic
$f_{GI}(x_1, x_2)$	0.92	0.75	0.85
$f_{large \rightarrow small}(x_1, x_2)$	<b>0.93</b>	0.64	0.85
$f_{small \rightarrow large}(x_1, x_2)$	0.84	0.66	0.81
$f_{mean}(x_1, x_2)$	<b>0.93</b>	<b>0.78</b>	<b>0.88</b>
$f_{geary}(x_1, x_2)$	0.88	0.71	0.83
$f_{bliss}(x_1, x_2)$	0.85	0.43	0.86

Table 7: AUC analysis on lack-of-fit method applied to Cokol dataset.

	synergistic	non-interactive	antagonistic
$f_{GI}(x_1, x_2)$	0.40	<b>0.70</b>	0.29
$f_{large \rightarrow small}(x_1, x_2)$	0.42	0.64	<b>0.37</b>
$f_{small \rightarrow large}(x_1, x_2)$	0.47	0.64	0.14
$f_{mean}(x_1, x_2)$	0.50	0.69	0.10
$f_{geary}(x_1, x_2)$	<b>0.60</b>	0.65	0.14
$f_{bliss}(x_1, x_2)$	0.40	0.53	0.17

Table 8: PRC-AUC analysis on parametric method applied to Mathews Griner dataset.

	synergistic	non-interactive	antagonistic
$f_{GI}(x_1, x_2)$	0.81	0.77	0.41
$f_{large \rightarrow small}(x_1, x_2)$	<b>0.82</b>	0.77	<b>0.50</b>
$f_{small \rightarrow large}(x_1, x_2)$	0.75	0.73	0.33
$f_{mean}(x_1, x_2)$	0.81	<b>0.78</b>	0.38
$f_{geary}(x_1, x_2)$	0.72	0.73	0.34
$f_{bliss}(x_1, x_2)$	0.55	0.66	0.38

Table 9: PRC-AUC analysis on lack-of-fit method applied to Mathews Griner dataset.

	synergistic	non-interactive	antagonistic
$f_{GI}(x_1, x_2)$	0.38	<b>0.61</b>	0.52
$f_{large \rightarrow small}(x_1, x_2)$	0.66	0.50	<b>0.71</b>
$f_{small \rightarrow large}(x_1, x_2)$	0.50	0.44	0.44
$f_{mean}(x_1, x_2)$	<b>0.69</b>	0.49	0.60
$f_{geary}(x_1, x_2)$	0.58	0.49	0.64
$f_{bliss}(x_1, x_2)$	0.30	0.48	0.50

Table 10: PRC-AUC analysis on parametric method applied to Cokol dataset.

	synergistic	non-interactive	antagonistic
$f_{GI}(x_1, x_2)$	0.80	0.63	0.78
$f_{large \rightarrow small}(x_1, x_2)$	0.83	0.49	0.75
$f_{small \rightarrow large}(x_1, x_2)$	0.67	0.55	0.69
$f_{mean}(x_1, x_2)$	<b>0.84</b>	<b>0.67</b>	<b>0.82</b>
$f_{geary}(x_1, x_2)$	0.76	0.58	0.74
$f_{bliss}(x_1, x_2)$	0.69	0.35	0.69

Table 11: PRC-AUC analysis on lack-of-fit method applied to Cokol dataset.